analytical chemistry

Article

pubs.acs.org/ac

Detection of Intracellular Selenol-Containing Molecules Using a Fluorescent Probe with Near-Zero Background Signal

Qi Sun,[†,§] Shu-Hou Yang,[†,§] Lei Wu,[†] Qing-Jian Dong,[‡] Wen-Chao Yang,*[,†] and Guang-Fu Yang*[,†]

[†]Key Laboratory of Pesticide & Chemical Biology of Ministry of Education, College of Chemistry, Central China Normal University, Wuhan 430079, P.R. China

[‡]Department of Nuclear Medicine, Tongji Hospital, Tongji Medical College, Huazhong University of Science and Technology, Wuhan 430030, P.R. China

Supporting Information

ABSTRACT: Selenocysteine (Sec), encoded as the 21st amino acid, is the predominant chemical form of selenium that is closely related to various human diseases. Thus, it is of high importance to identify novel probes for sensitive and selective recognition of Sec and Sec-containing proteins. Although a few probes have been reported to detect artificially introduced selenols in cells or tissues, none of them has been shown to be sensitive enough to detect endogenous selenols. We report the characterization and application of a new fluorogenic molecular probe for the detection of intracellular selenols. This probe exhibits near-zero background fluorescence but produces remarkable fluorescence enhancement upon reacting with selenols in a fast chemical reaction. It is highly specific and sensitive for intracellular selenium-containing molecules such as Sec and selenoproteins. When combined with flow cytometry, this probe is able to detect endogenous selenols in various human cancer cells. It is also able to image endogenous selenol-containing molecules in zebrafish under a fluorescence microscope. These results demonstrate that this molecular probe can function as a useful molecular tool for intracellular selenol sensing, which is valuable in the clinical diagnosis for human diseases associated with Sec-deficiency or overdose.

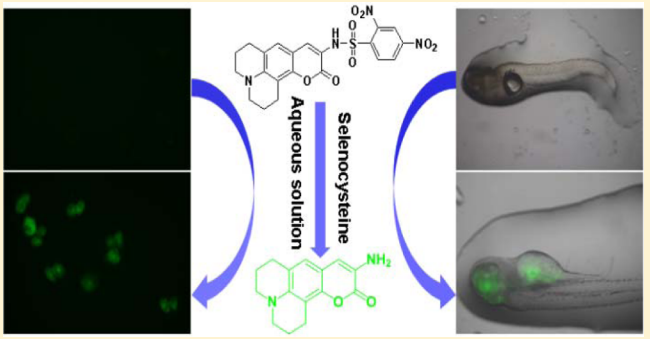

Selenium, discovered in 1817, is a micronutrient known to be important to human health.[1−7] The year 2017 was announced to be the selenium year in recognition of the significance of selenium for 200 years. Intracellular selenium mainly takes the form of selenocysteine (Sec),[8,9] which is an essential building block for selenoproteins (SePs).[10−16] SePs have been implicated in various cellular functions and linked to several human diseases, such as cancers, cardiovascular diseases, neurodegenerative diseases, and inflammations.[6,17−21] Due to the importance of biological selenols, there is a growing interest in developing highly selective fluorescent molecular probes that can facilitate intracellular selenol-containing molecule detection and creation of molecular tools to diagnose human diseases associated with selenium deficiency and overdose.[22−25] However, designing selenol-selective probes represents a significant challenge mostly due to the interference of biological thiols that share similar chemical properties to selenols but are much more abundant in cells and other biological samples. To date, only a few fluorescent probes have been designed to selectively detect biological selenols.[22,24,26] Although these probes are able to detect artificially introduced selenols in cells or tissues (thus at significantly elevated levels), none of them has been shown to be sensitive enough to detect endogenous selenols, an important issue that we sought to solve in the current study.

The selenol pK_a value in Sec (∼5.8) is lower than thiophenol (∼6.5) and biological thiols (∼8.3), which means Sec is more likely to exist as deprotonated state. So, the thiophenol probe may also react with Sec in acidic conditions due to the same mechanism of nucleophilic attack. We have previously reported a thiophenol probe, denoted **1**, that is only weakly fluorescent (quantum yield Φ = 0.0050).[27] Probe **1** indeed reacted with selenol, such as Sec, resulting in the release of the free fluorophore, 7-*N*, *N*-diethylaminocoumarin (**2**). Because the quantum yield (Φ) of **2** is 0.14, this reaction leads to the generation of a strong fluorescence. Probe **1** shows excellent selectivity and sensitivity for Sec, with a limit of detection (LOD) of ∼62 nM.[26] It is sensitive enough for quantifying the serum concentration of selenium in healthy adults (>500 nM), but it is not sufficient for accurate selenium determination in the selenium-deficient patients with Keshan disease or Kashin−Beck disease (∼100 nM).[20,28,29] Therefore, further modification

Received: April 19, 2016
Accepted: May 10, 2016
Published: May 10, 2016

DOI: 10.1021/acs.analchem.6b01545
Anal. Chem. 2016, 88, 6084−6091

of probe **1** is necessary in order to further improve its detection sensitivity.

Recently, we hypothesized that the blockage of internal twisting of the nitrogen atom at 7-position on the coumarin ring of probe **1** can significantly enhance the quantum yield of the freed fluorophore, and we then discovered a new thiophenol probe with improved sensitivity through the strategy of blocking the internal twisting of the nitrogen atom at 7-position on coumarin ring (denoted **3** in Scheme 1).[30]

Scheme 1. Mechanism of Sec Detection with Molecular Probe 3

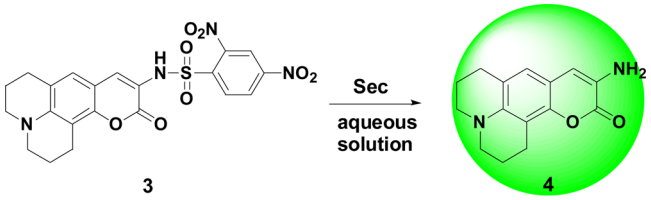

Inspired by the good detection capability against selenol with thiophenol probe **1**, the newly developed probe **3** was applied for selenol-containing molecule detection in this study. After comprehensive characterization, the new probe shows much improved properties for selenol-containing molecules: (1) exhibits a first-order rate constant (k) of 2.15 min^{-1}, the best among all reported Sec probes to date; (2) about 250-fold fluorescence intensity enhancement in pure aqueous solution; and (3) sufficient LOD (~18 nM) for selenium determination in selenium-deficient patients. More importantly, probe **3** is able to detect intracellular selenols with flow cytometry and to discriminate the cancer cells from normal cells. To the best of our knowledge, this is the first report that cancer cells showed higher intracellular level of selenol-containing molecules compared to normal cells. In addition, the probe successfully imaged the endogenous selenol-containing molecule and exogenous Sec in zebrafish, demonstrating its potential for the biological function study of SePs and the clinical diagnosis for the selenium-related diseases.

EXPERIMENTAL SECTION

Organic Synthesis. Unless otherwise noted, all chemical reagents were commercially available and treated with standard methods before use. Silica gel column chromatography (CC): silica gel (200−300 mesh); Qingdao Makall Group Co., Ltd. (Qingdao; China). Solvents were dried in a routine way and redistilled. ^{1}H NMR was recorded in DMSO-d_6 or $CDCl_3$ on a Varian Mercury 400 and 600 MHz spectrometer, whereas the ^{13}C NMR spectra were recorded at 100 and 150 MHz spectrometer. The resonances (δ) are given in ppm relative to tetramethylsilane (TMS). The following abbreviations were used to designate chemical shift mutiplicities: s = singlet, d = doublet, t = triplet, m = multiplet, br = broad. High-resolution mass spectra (HRMS) were acquired in positive mode on a WATERS MALDI SYNAPT G2 HDMS (MA, U.S.A.). Melting points were taken on a Buchi B-545 melting point apparatus and uncorrected.

Synthesis of Probe 3. The major intermediates (**M** and **4**) and the final product (probe **3**) were synthesized according to reported methods.[31−33]

*(10-Nitro-2,3,6,7-tetrahydro-1H,5H,11H-pyrano[2,3-f]-pyrido[3,2,1-ij]quinolin-11-one) (**M**).* Purple solid, yield: 77%, ^{1}H NMR (400 MHz, $CDCl_3$): δ 8.55 (s, 1H), 6.98 (s, 1H), 3.41 (q, J = 5.3 Hz, 4H), 2.76−2.86 (m, 4H), 1.99 (s, 4H).

*(10-Amino-2,3,6,7-tetrahydro-1H,5H,11H-pyrano[2,3-f]-pyrido[3,2,1-ij] quinolin-11-one) (**4**).* Yellow solid, yield: 61%, ^{1}H NMR (400 MHz, DMSO-d_6): δ 6.79 (s, 1H), 6.62 (s, 1H), 4.97 (s, 2H), 3.11−3.14 (m, 4H), 2.67−2.74 (m, 4H), 1.85−1.91 (m, 4H). HRMS calcd for [M^+]: 256.1206. Found: 256.1211.

*(2,4-Dinitro-N-(11-oxo-2,3,6,7-tetrahydro-1H,5H,11H-pyrano[2,3-f]pyrido[3,2,1-ij]quinolin-10-yl)-benzenesulfonamide) (Probe **3**).* Black solid, yield: 86%. mp: 206−207 °C. ^{1}H NMR (600 MHz, $CDCl_3$): δ 8.76 (d, J = 1.8 Hz, 1H), 8.41 (d, J = 6 Hz, 1H), 8.13 (d, J = 8.4 Hz, 1H), 7.78 (d, J = 3.6 Hz, 2H), 6.94 (s, 1H), 3.25−3.30 (m, 4H), 2.77 (q, J = 8.0 Hz, 4H), 1.92−1.98 (m, 4H). ^{13}C NMR (100 MHz, DMSO-d_6): δ 164.32, 154.90, 154.65, 152.34, 150.94, 145.58, 142.95, 137.05, 131.84, 130.54, 124.59, 123.66, 118.07, 111.83, 110.16, 59.78, 54.22, 53.69, 31.72, 25.68, 24.65. HRMS calcd for [M + H]$^+$: 487.0918. Found: 487.0914. Anal. Calcd for $C_{21}H_{18}N_4O_8S$: C, 51.85; H, 3.73; N, 11.52; S, 6.59; Found: C, 51.82; H, 3.72; N, 11.53; S, 6.56.

Sec Sensing and Selectivity Evaluation. The sensing reaction of probe **3** (10 μM) with a certain amount of Sec was carried out in 100 mM phosphate buffer at the desired pH environment at 30 °C. The Sec was freshly prepared by the preincubation of equimolar $(Sec)_2$ with DTT in the same phosphate buffer. The fluorescence intensity of the above system was monitored at the wavelength of 535 nm (λ_{ex} = 380 nm).

To study the interference that may be caused by small molecules or ions, probe **3** (10 μM) was mixed with various analytes, such as amino acids (Phe, Arg, His, Tyr, Ala, Trp, Lys, and Met), metal ions (Ca^{2+}, Mg^{2+}, Na^+, and K^+), and biological thiols (Cys, Hcy, and GSH), respectively. After 30 min of incubation, the fluorescence intensity of each sample was measured at the wavelength of 535 nm (λ_{ex} = 380 nm). Similar selectivity studies were performed against protein and enzymes (bovine serum albumin (BSA), human elastase, acetylcholinesterase (AChE), butyrylcholinesterase (BChE), and trypsin), and their final concentrations were around 0.01 mg/mL, whereas the concentration of recombinant human thioredoxin-inredutase (hTR) is about 0.01 mg/mL. The fold of fluorescence increase (F/F_0) was normalized to the base fluorescence intensity of probe **3** for the above studies.

The recombinant hTR was generated by overexpression of hTR-pGEX plasmid that was purchased form Protech Company (Wuhan, China). The mutants U498C and U498S were obtained by site-directed mutagenesis.

Determination of Quantum Yield. According to the reported method, the quantum yields for probe **3** and its fluorophore (compound **4**) were determined with rhodamine B as reference.[27,34,35] More specifically, using rhodamine B (Φ = 0.88, ethanol) as reference, compounds **3** and **4** were first diluted to suitable concentration by PBS (0.1 M, pH 7.0) buffer to make their absorption less than 0.05. Then, their absorbance and integral areas were studied at this concentration. Finally, the quantum yields of these two compounds were calculated by Abbe's refractometer and the following equation.

$$\phi_s = \frac{F_s \cdot A_c}{F_c \cdot A_s}\phi_c \quad (1)$$

DOI: 10.1021/acs.analchem.6b01545
Anal. Chem. 2016, 88, 6084−6091

Determination of Second-Order Reaction Rate Constant. For a second-order reaction, A and B are reactants, whereas the C and D are products.

$$A + B \xrightarrow{k} C + D$$

If the starting concentrations of compound A and B are equal, such as a, the reaction rate can be calculated by the following equation. K is the second order reaction rate, x means the concentrations of products, such as C and D.

$$\frac{dx}{dt} = K \times (a - x)^2 \quad (2)$$

Then the eq 3 was converted from eq 2.

$$\frac{1}{a - x} = K \times t \quad (3)$$

For our system, the fluorescence intensity F and concentration of products are in the linear relationship at the early stage. So the concentration of the product can be calculated by the eq 4

$$x = \frac{F_t - F_0}{F_\infty - F_t} \times a \quad (4)$$

In the above equation, F_0 represent the start fluorescence intensity of reaction systems at $t = 0$. F_∞ represent the total fluorescence intensity of reaction systems when the reaction had been completed. F_t means the fluorescence intensity of reaction systems after incubation time t. The fluorescence intensity of reaction systems was monitored at the wavelength of 535 nm (λ_{ex} = 380 nm).

The eq 4 was substituted into eq 3 to yield the eq 5. On the basis of this equation, the second-order reaction rate K could be calculated.

$$\frac{F_t - F_0}{F_\infty - F_t} = K \times a \times t \quad (5)$$

Living Cell Imaging and Cytotoxicity Study. H460 cells were cultured in DMEM supplemented with 10% (v/v) fetal bovine serum, 1% (v/v) penicillin/streptomycin and maintained in the atmosphere of 5% CO_2 at 37 °C. The cells were seeded on 6-well plates at 1×10^5 cells per well in 2 mL of culture medium and incubated overnight in 5% CO_2 at 37 °C. Then both $(Sec)_2$ and DTT (20 μM) were added into the cells and incubated for different times (0, 6, and 12 h). After washing the cells with PBS three times to move the remaining $(Sec)_2$ and DTT,the cells were further incubated with probe **3** (20 μM) for 20 min at 37 °C. After washing the cells with PBS three times, the treated cells were imaged by inverted fluorescence microscopy (Olympus IX71, Japan). In order to induce endogenous Sec, the H460 cells were treated with sodium selenite (20 μM) for different times (0, 6 and 12 h). Then the cells were incubated with the probe **3** (20 μM) for 20 min at 37 °C. After the cells were washed three times to remove the remaining probe **3**, the fluorescence images were acquired with inverted fluorescence microscopy. In the meantime, the control group was incubated with only the probe **3** (20 μM) for different times (0, 6, and 12 h) at 37 °C and then imaged by microscopy.

To study the cytotoxicity, HEK293 cells were seeded at 1×10^5 cells per well in 96-well plates and incubated for 24 h before treatment, followed by exposure to different concentrations (0, 1, 5, 10, 20, 50 μM) of probe **3**, Sec, Na_2SeO_3, and compound **4** for an additional 24 h. To determine the cell viability, the colorimetric assay with 3-(4, 5-dimethylthiazol-2-yl)-3, 5-diphenytetrazolium bromide (MTT) was applied for evaluating the metabolic activity. Cell samples were incubated with MTT solution (containing 5 mg/mL MTT reagent in PBS) for 4 h, and then, DMSO was added to dissolve the formazan crystals after removal of the MTT solution. The absorbance was measured at 540 nm with a microplate reader (SpectraMax M5, Molecular Devices). Each experiment was performed at least three times. The cytotoxic effect was evaluated accordingly.

Flow Cytometry Analysis. Flow cytometry (C6, BD Biosciences) was employed to determine endogenous selenol with the developed probe. Cancer and normal cell cultures were prepared for sample analysis. After removing media and rinsing with PBS buffer, the cells were treated with trypsin (0.25%). The digested cells were centrifugated and further suspended at a density of 2×10^5/mL with PBS in 1.5 mL eppendorf tubes. Following treatment with a range of concentrations (0, 0.1, 1, 10, and 100 μM) of probe **3** at room temperature for 10 min, the fluorescence signal was determined in a FL1-A detector by flow cytometry. Analysis was conducted for a minimum of 10 000 counting events, and median values of histograms were used to quantify the Sec recognition with probe **3**.

***In Vivo* Imaging of Zebrafish.** To explore the potential of probe **3** as an *in vivo* imaging tool, we applied it to detection in living zebrafish. Zebrafish, which are 3−7 days postfertilization, were purchased from Eze-Rinka Company (Nanjing, China). The zebrafish were cultured in 5 mL of embryo medium supplemented with 1-phenyl-2-thiourea (PTU) in 6-well plates for 24 h at 30 °C. Then the zebrafish embryos were washed three times to remove the remaining $(Sec)_2$ and DTT, and they were further incubated with probe **3** (10 μM) for 24 h at 30 °C. After removing the embryo medium and washing the zebrafish with PBS for three times, the fluorescence images were acquired with stereomicroscopy (Olympus SZX16, Japan). In order to detect endogenous selenol contents, the zebrafish were directly treated with embryo medium containing probe **3** (10 μM) for 24 h. After washing the zebrafish for three times, the zebrafish were imaged by stereo microscopy. As the negative control, the zebrafish without any treatment were imaged directly.

RESULTS AND DISCUSSION

Probe Synthesis. The new probe **3** was prepared in three steps, and the detailed synthetic route is shown in Scheme 2. The structures of probe **3** and intermediate molecules were

Scheme 2. Synthetic Route of Probe 3

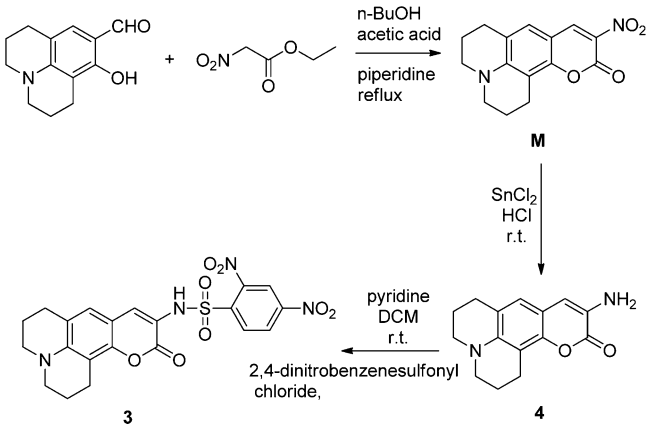

DOI: 10.1021/acs.analchem.6b01545
Anal. Chem. 2016, 88, 6084−6091

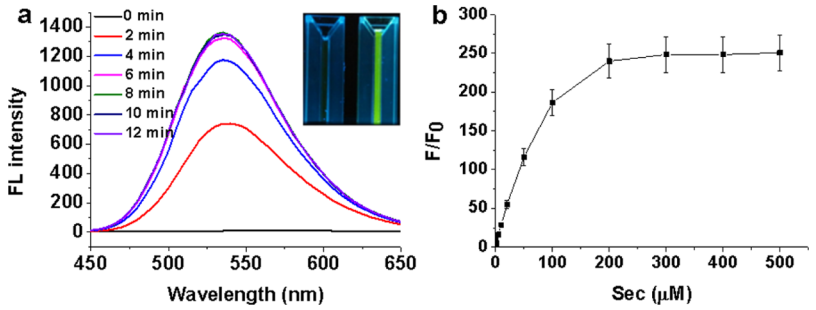

Figure 1. (a) Time dependence for the fluorescence spectra (λ_{ex} = 380 nm) of probe **3** (10 μM) in the presence of Sec (50 μM) in 0.1 M phosphate buffer (pH 7.0) at 30 °C. Inset: photo of samples illuminated with 365 nm UV light with and without the addition of Sec (50 μM). (b) The change of the relative fluorescence intensity (F/F_0) at 535 nm of the probe **3** (10 μM) with increasing concentrations of Sec.

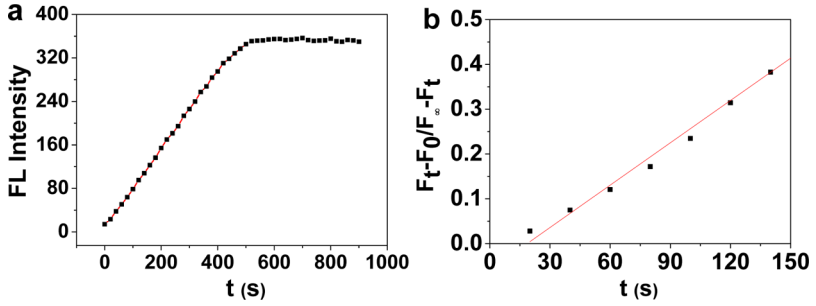

Figure 2. (a) Time dependence for the fluorescence spectra (λ_{em} = 515 nm) of probe **3** (10 μM) in the presence of Sec (10 μM) in 0.1 M phosphate buffer (pH 7.0) at 30 °C. (b) The plot of the reaction progress ($(F_t - F_0)/(F_\infty - F_t)$) vs the reaction time. F_0 is the initial fluorescence intensity of reaction system, F_t is the fluorescence intensity of reaction system at the corresponding time, F_∞ is the total fluorescence intensity when 100% substrate converted, and t is incubation time in seconds.

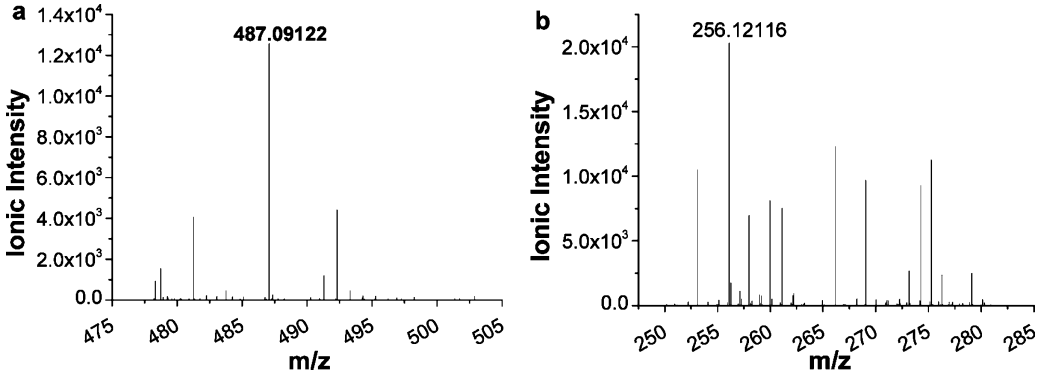

Figure 3. HPLC-MS spectrum of pure probe **3** (a), and the reaction system between probe **3** and Sec. Molecular ion mass peak of (a) [**3** + H^+] (calcd. for 487.0918), (b) $[\mathbf{4}]^+$ (calcd. for 256.1206).

fully characterized (see Figure S1−S6). The water solubility of probe **3** was investigated prior to the fluorescence property characterization. It revealed that the maximum absorbance in 0.1 M phosphate buffer (pH 7.4) linearly increased with increasing the concentration of probe **3** (0−200 μM, see Figure S7), indicating good water solubility of the newly synthesized probe. Thus, probe **3** is readily soluble in phosphate buffer system, and there is no need for cosolvent for biological selenol-containing molecule detection.

Fluorescence, pH Dependence, and Sensitivity of Probe 3. Based on the primary characterization, probe **3** exhibits several very desirable properties in pure aqueous solution (Figure 1). First, the new probe has near zero fluorescence background (Φ = 0.0014). Second, molecule **4**, the fluorophore of probe **3**, has an increased quantum yield (0.30; in comparison, Φ of **2** is 0.14) and a notable red shift (λ_{ex}= 380 nm and λ_{em}= 535 nm; Figure S8). Third, probe **3** exhibits a first-order rate constant (k) of 2.15 min^{-1} when reacting with 10 times higher concentration of Sec at 30 °C (Figure 2a), the best for all reported Sec probes to date (for comparison, k is ∼1.34 min^{-1} for Sel-green at 30 °C and ∼0.16 min^{-1} for HD-Sec at 25 °C).[24,26] To compare with the reported selenol probe[22] with a second-order rate constant of 740 $M^{-1}\cdot s^{-1}$ at 37 °C, the second-order rate constant of probe **3** reacting with Sec was measured at 30 °C (Figure 3). The second-order rate constant at 30 °C was calculated to be ∼700 $M^{-1}\cdot s^{-1}$ by eq 5, which should be even higher at 37 °C. In addition, the Sec-reactivity of probe **3** has a bell-shaped pH dependence (Figure S9), with the maximal value at pH 6.0. On the basis of this observation, pH 6.0 was chosen for the remaining experiments in this study. From the concentration titration experiment shown in Figure S10 and Figure 2b, Sec can produce up to 250-

DOI: 10.1021/acs.analchem.6b01545
Anal. Chem. 2016, 88, 6084−6091

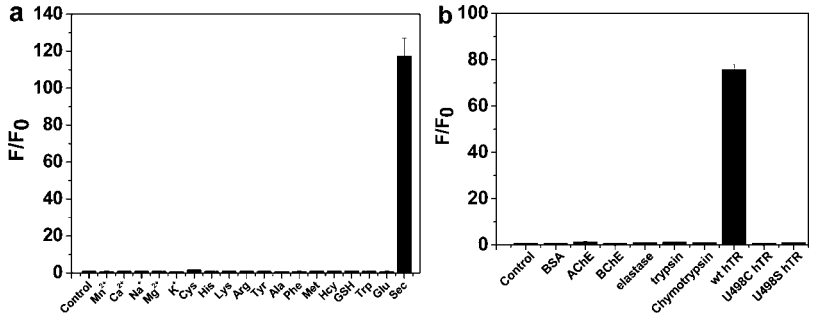

Figure 4. (a) Selectivity profile of probe **3** against metal ions, amino acids, biological thiols, and Sec. F/F_0 represents the relative fluorescence response. The probe concentration was 10 μM, the Sec concentration was 100 μM, and other analytes were added at 1000 μM. (b) The selectivity profile of probe **3** against hTR (1 μg/mL) and proteins (10 μg/mL) that do not have Sec residue. F/F_0 represents the relative fluorescence response. The probe concentration was 10 μM.

fold fluorescence enhancement. On the basis of the calibration curve of response of probe **3** to Sec in aqueous solution, the LOD for Sec is further determined to be about 18 nM (Figure S11).

It is noteworthy that the turn-on fluorescence sensing mechanism of probe **3** upon the recognition of Sec was validated by HRMS and HLC analyses. As the reference, Figure 3a shows the HRMS peak of the probe [**3** + H^+] (calcd. for 487.0918) before the addition of Sec. When monitoring the reaction system of probe **3** and Sec, which are solved in dd-water containing 0.1% (v/v) DMSO (the final concentration are 20 μM), the HRMS peak of compound **4** (calcd. for 256.1206) was also found in Figure 3b. To further validate this reaction mechanism, the reaction of probe **3** in the absence and presence of Sec was monitored by HPLC, with fluorophore (**4**) as reference (Figure S12). All of them were solved in CH_3CN, the mobile phase (ACN:H_2O) is 60%:40%, and the flow rate is 0.3 mL/min. It shows that the signal peak of reaction system between probe **3** and Sec correlates well with the signal peaks of the fluorophore (**4**). These results indicate that probe **3** actually reacted with Sec and gave out **4** as a product.

Probe Selectivity. We tested the selectivity profile of probe **3**. The data presented in Figure 4a shows that this molecular probe is highly selective for selenols (represented by Sec) over competing amino acids (Phe, Arg, His, Tyr, Trp, Ala, Lys, and Met), metal ions (Ca^{2+}, Mg^{2+}, Na^+, and K^+) and biothiols (Cys, Hcy, and GSH). It displayed 120-fold fluorescence enhancement upon treatment with Sec, indicating that probe **3** is particularly selective toward Sec. We also tested the reactivity of probe **3** with SePs. We chose human thioredoxin redutase (hTR), a well-characterized human SeP for this examination. It is known that hTR contains a single Sec residue locating at the C terminal. We prepared and tested the recombinant version of hTR (1 μg/mL), as well as two hTR mutants, U498C and U498S, in which Sec was substituted with cysteine and serine, respectively. In addition, we also tested five control proteins (10 μg/mL)—bovine serum albumin (BSA), human elastase, acetylcholinesterase (AChE), butyrylcholinesterase (BChE) and trypsin—that do not contain Sec but commonly exist in serum. As shown in Figure 4b, only wild-type hTR (wt hTR) was able to produce significant fluorescence enhancement, indicating our molecular probe is able to selectively detect SePs. In addition, the second-order reaction rate constant for the reaction between probe **3** and hTR was measured to be about 1200 $M^{-1}\cdot s^{-1}$. Thus, the reaction between probe **3** and hTR was only slightly faster than that of reaction between probe **3** and Sec (700 $M^{-1}\cdot s^{-1}$) at 30 °C, which indicates that the probe 3 could not discriminate the hTR and Sec.

Cytotoxity of Probe 3 and Its Application in Cell Imaging. We next carried out an imaging study using probe **3** against human lung cancer cells (A549). We first studied the response of probe **3** to the exogenous Sec in cells at different time points. After treated with Sec newly prepared by an equimolar complex of $(Sec)_2$ and DTT to the cultured cells, a bright and strong green fluorescence could be observed after 6 h, and the green fluorescence became stronger after 12 h; however, there was no significant fluorescence signal in control cells througout the entire duration (Figure 5a,c). We also examined the cells treated with sodium selenium (Na_2SeO_3), a classical precursor of Sec biosynthesis. It was expected that the cells treated with Na_2SeO_3 would produce increased level of reactive selenol species. This was confirmed by the data presented in Figure 5b, and the green fluorescence also

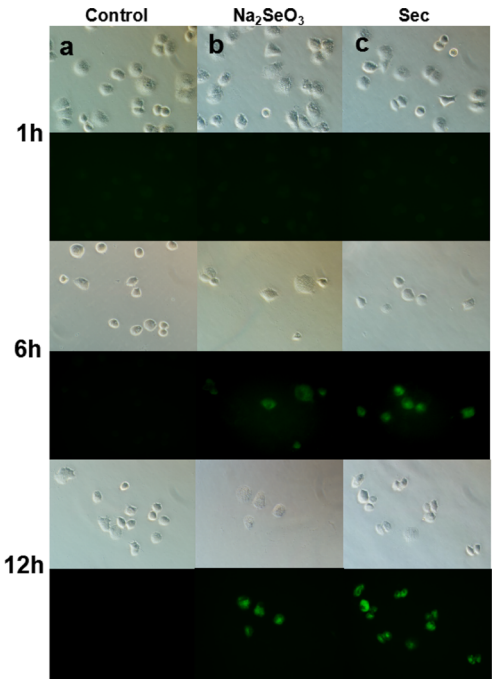

Figure 5. Fluorescence imaging in A549 cells at different incubation times (0, 6, and 12 h). The cells were untreated (a), with 20 μM Na_2SeO_3 (b), and treated with 20 μM $(Sec)_2$ and 20 μM DTT(c), and the bright-field images (top panel of each time point), fluorescence images (bottom panel of each time point) were acquired.

DOI: 10.1021/acs.analchem.6b01545
Anal. Chem. 2016, 88, 6084−6091

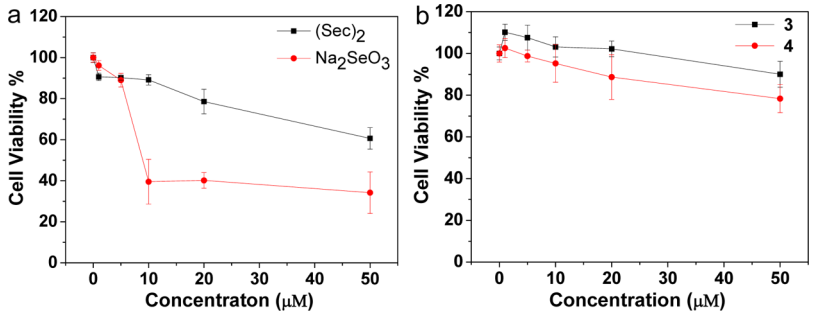

Figure 6. Cytotoxicity of representative selenocompounds (a) and new synthesized compounds (b) against HEK293 cells. The cell viability was determined by the MTT assay. Data represent average values of three independent experiments.

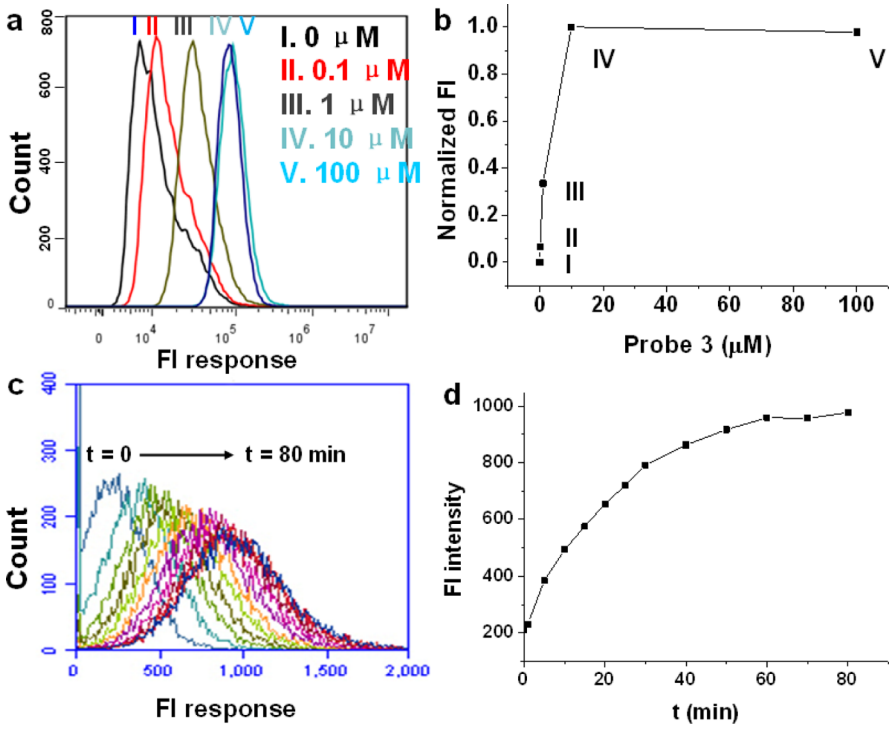

Figure 7. (a) Flow cytometric analysis of A549 cells exposed to different concentrations of probe **3** (I, 0 μM; II, 0.1 μM; III, 1 μM; IV, 10 μM; V, 100 μM) after 10 min incubation. (b) Plot of the fluorescence signal versus the probe concentration in flow cytometry. (c) The flow cytometric analysis of A549 cells exposed to probe **3** (10 μM) after different time of incubation. (d) Plot of the fluorescence signal versus the incubation time in flow cytometry.

increased with the extension of the incubation time. These results show that probe **3** is capable of detecting purposely elevated Sec in mammalian cells. In addition, the results obtained from the MTT assay indicated that probe **3** and its fluorophore did not cause significant cytotoxicity against HEK293 cells, whereas the representative selenocompounds, Sec and Na_2SeO_3, caused severe cytotoxicity (see Figure 6).

Endogenous Cellular Selenol/Sec Determination. We then examined whether probe **3** was useful for detecting endogenous selenols in single cells using flow cytometry. Probe **3** was tested at four different concentrations (0.1, 1, 10, and 100 μM) with A549, a lung cancer cell. The results depicted in Figure 7a (as well as Figure S13) and the resultant plot of the fluorescence intensity versus the concentration of probe **3** were shown in Figure 7b. Moreover, the time-dependent profile of the fluorescence for A549 cells was investigated, and the corresponding results were shown in Figure 7c,d. Notably, those data demonstrate that probe **3** can indeed detect intracellular selenols in individual cells, reaching the highest signal at 10 μM of probe and a cell-probe incubation time of 10 min.

The above flow-cytometry-based method was further used to measure the relative selenol concentrations by probe **3** in both normal cells (HEK293 and COS) and three cancer cell lines (A549, H460, and HeLa). Interestingly, the data presented in Figure 8 revealed that selenol levels in the chosen cancer cells are noticeably higher than that of normal cells, a novel observation that has never been described before.

***In Vivo* Selenol/Sec Imaging of Zebrafish with Probe 3.** We also investigated the suitability of probe **3** as *in vivo* imaging agent. Zebrafish were chosen for this investigation mainly for experimental simplicity (they can be conveniently imaged under fluorescence microscopy).[36,37] Zebrafish were divided into three groups: the control group (group a in Figure 9; no probe **3** added), the intrinsic selenol test group (group b in Figure 9, treated with probe **3** alone), and the chemically enhanced selenol test group (group c in Figure 9, treated with probe **3** as well as equimolar complex of $(Sec)_2$ and DTT to

DOI: 10.1021/acs.analchem.6b01545
Anal. Chem. 2016, 88, 6084−6091

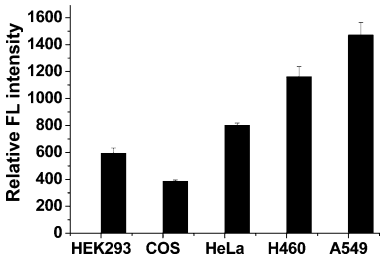

Figure 8. Flow cytometric analysis of normal cells (HEK293 and COS) and cancer cells with probe **3** (10 μM).

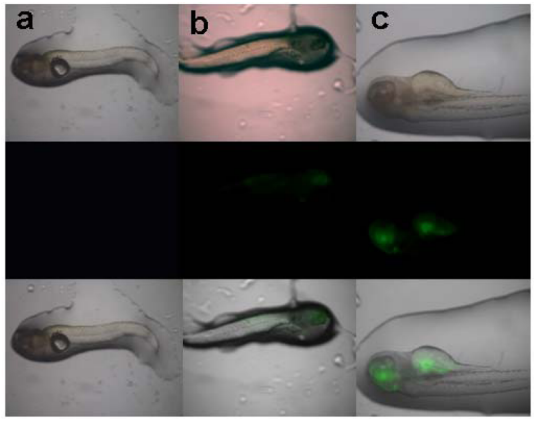

Figure 9. Confocal imaging of selenols in zebrafish embryos, 30 min after incubation of probe **3**: (a) Control group (no probe), (b) Probe group (only 10 μM probe **3** was added), (c) Sample group (10 μM probe **3**, 20 μM $(Sec)_2$ and 20 μM DTT were added).

produce enhanced level of selenols). No significant fluorescence was observed in the control group. However, probe **3** was able to detect both intracellular selenol-containing molecules in the intrinsic selenol group b (strong fluorescence was observed in the head) and chemically enhanced selenol group c (strong fluorescence was seen in both the head and the venter). These results demonstrate that probe **3** can perform sensitive Sec imaging in the living organisms.

CONCLUSION

In conclusion, we have successfully identified a new molecular probe for selenol-containing molecule recognition. This probe exhibits several very desirable properties, including near-zero background fluorescence, large fluorescence enhancement upon reacting with Sec (~250-fold), a low LOD (18 nM), and a large Sec-reacting rate constant (~2.15 min^{-1}). Furthermore, probe **3** can be used to carry out sensitive intracellular selenol-containing molecule detection using live cells and living organisms. We expect this molecular probe can find useful applications both in the study of biological function related to SePs and in the clinical diagnosis for human diseases associated with Se-deficiency or overdose.

ASSOCIATED CONTENT

Supporting Information

The Supporting Information is available free of charge on the ACS Publications website at DOI: 10.1021/acs.analchem.6b01545.

NMR, LC-MS, and HPLC spectra for the newly synthesized compounds, and selected figures for probe **3** characterization (PDF)

AUTHOR INFORMATION

Corresponding Authors

*E-mail for W.-C.Y.: tomyang@mail.ccnu.edu.cn. Tel: 86-27-67867706. Fax: 86-27-67867141.

*E-mail for G.-F.Y.: gfyang@mail.ccnu.edu.cn. Tel: 86-27-67867800. Fax: 86-27-67867141.

Author Contributions

§These authors contributed equally (Q.S. and S.-H.Y.).

Notes

The authors declare no competing financial interest.

ACKNOWLEDGMENTS

We are grateful for the financial support from the National Natural Science Foundation of China (Grant Nos. 21332004 and 21372094).

REFERENCES

(1) Foster, L. H.; Sumar, S. *Crit. Rev. Food Sci. Nutr.* **1997**, *37*, 211−228.
(2) Rayman, M. P. *Lancet* **2000**, *356*, 233−241.
(3) Chen, J.; Berry, M. J. *J. Neurochem.* **2003**, *86*, 1−12.
(4) Thomson, C. D. *Eur. J. Clin. Nutr.* **2004**, *58*, 391−402.
(5) Duntas, L. H.; Benvenga, S. *Endocrine* **2015**, *48*, 756−775.
(6) Du, X.; Wang, C.; Liu, Q. *Curr. Top. Med. Chem.* **2016**, *16*, 835−848.
(7) Ogawa-Wong, A. N.; Berry, M. J.; Seale, L. A. *Nutrients* **2016**, *8*, 80−99.
(8) Weekley, C. M.; Harris, H. H. *Chem. Soc. Rev.* **2013**, *42*, 8870−8894.
(9) Hatfield, D. L.; Tsuji, P. A.; Carlson, B. A.; Gladyshev, V. N. *Trends Biochem. Sci.* **2014**, *39*, 112−120.
(10) Arthur, J. R. *Cell. Mol. Life Sci.* **2001**, *57*, 1825−1835.
(11) Hondal, R. J.; Nilsson, B. L.; Raines, R. T. *J. Am. Chem. Soc.* **2001**, *123*, 5140−5141.
(12) Kanzok, S. M.; Fechner, A.; Bauer, H.; Ulschmid, J. K.; Muller, H. M.; Botella-Munoz, J.; Schneuwly, S.; Schirmer, R.; Becker, K. *Science* **2001**, *291*, 643−646.
(13) Johansson, L.; Gafvelin, G.; Arner, E. S. J. *Biochim. Biophys. Acta, Gen. Subj.* **2005**, *1726*, 1−13.
(14) Bindoli, A.; Rigobello, M. P.; Scutari, G.; Gabbiani, C.; Casini, A.; Messori, L. *Coord. Chem. Rev.* **2009**, *253*, 1692−1707.
(15) Bela, K.; Horvath, E.; Galle, A.; Szabados, L.; Tari, I.; Csiszar, J. *J. Plant Physiol.* **2015**, *176*, 192−201.
(16) Darras, V. M.; Van Herck, S. L. *J. Endocrinol.* **2012**, *215*, 189−206.
(17) Kucharzewski, M.; Braziewicz, J.; Majewska, U.; Gozdz, S. *Biol. Trace Elem. Res.* **2002**, *88*, 25−30.
(18) Encinar, J. R.; Schaumloffel, D.; Ogra, Y.; Lobinski, R. *Anal. Chem.* **2004**, *76*, 6635−6642.
(19) Ballihaut, G.; Kilpatrick, L. E.; Davis, W. C. *Anal. Chem.* **2011**, *83*, 8667−8674.
(20) Fairweather-Tait, S. J.; Bao, Y.; Broadley, M. R.; Collings, R.; Ford, D.; Hesketh, J. E.; Hurst, R. *Antioxid. Redox Signaling* **2011**, *14*, 1337−1383.
(21) Tanguy, S.; Grauzam, S.; de Leiris, J.; Boucher, F. *Mol. Nutr. Food Res.* **2012**, *56*, 1106−1121.
(22) Maeda, H.; Katayama, K.; Matsuno, H.; Uno, T. *Angew. Chem., Int. Ed.* **2006**, *45*, 1810−1813.
(23) Yin, C. X.; Huo, F. J.; Zhang, J. J.; Martinez-Manez, R.; Yang, Y. T.; Lv, H. G.; Li, S. D. *Chem. Soc. Rev.* **2013**, *42*, 6032−6059.
(24) Chen, H.; Dong, B.; Tang, Y.; Lin, W. *Chem. - Eur. J.* **2015**, *21*, 11696−11700.

DOI: 10.1021/acs.analchem.6b01545
Anal. Chem. 2016, 88, 6084−6091

(25) Kong, F.; Hu, B.; Gao, Y.; Xu, K.; Pan, X.; Huang, F.; Zheng, Q.; Chen, H.; Tang, B. *Chem. Commun.* **2015**, *51*, 3102−3105.
(26) Zhang, B.; Ge, C.; Yao, J.; Liu, Y.; Xie, H.; Fang, J. *J. Am. Chem. Soc.* **2015**, *137*, 757−769.
(27) Li, J.; Zhang, C. F.; Yang, S. H.; Yang, W. C.; Yang, G. F. *Anal. Chem.* **2014**, *86*, 3037−3042.
(28) World Health Organization. *Vitamin and mineral requirements in human nutrition*, 2nd ed.; World Health Organization, Food and Agriculture Organization of the United Nations: Geneva, Switzerland, 2004.
(29) *Selenium deficiency and toxicity in the environment in Essentials of medical geology: impacts of the natural environment on public health*; Selinus, O., Alloway, B. J., Eds.; Elsevier Academic Press: Amsterdam, 2005.
(30) Sun, Q.; Yang, S. H.; Wu, L.; Yang, W. C.; Yang, G. F. *Anal. Chem.* **2016**, *88*, 2266−2272.
(31) Van Gompel, J.; Schuster, G. B. *J. Org. Chem.* **1987**, *52*, 1465−1468.
(32) Lee, S.; Sivakumar, K.; Shin, W. S.; Xie, F.; Wang, Q. *Bioorg. Med. Chem. Lett.* **2006**, *16*, 4596−4599.
(33) Sun, Q.; Yang, S. H.; Wu, L.; Yang, W. C.; Yang, G. F. *Anal. Chem.* **2016**, *88*, 2266−2272.
(34) Qian, F.; Zhang, C.; Zhang, Y.; He, W.; Gao, X.; Hu, P.; Guo, Z. *J. Am. Chem. Soc.* **2009**, *131*, 1460−1468.
(35) Sun, Q.; Li, J.; Liu, W. N.; Dong, Q. J.; Yang, W. C.; Yang, G. F. *Anal. Chem.* **2013**, *85*, 11304−11311.
(36) Xu, Z.; Baek, K. H.; Kim, H. N.; Cui, J.; Qian, X.; Spring, D. R.; Shin, I.; Yoon, J. *J. Am. Chem. Soc.* **2010**, *132*, 601−610.
(37) Hu, J. J.; Wong, N. K.; Ye, S.; Chen, X.; Lu, M. Y.; Zhao, A. Q.; Guo, Y.; Ma, A. C.; Leung, A. Y.; Shen, J.; Yang, D. *J. Am. Chem. Soc.* **2015**, *137*, 6837−6843.

DOI: 10.1021/acs.analchem.6b01545
Anal. Chem. 2016, 88, 6084−6091